Vortex-related phase-transition-like behavior in the electrical properties of *c*-axis normal and vicinal $YBa_2Cu_3O_{7-\delta}$ films

P. S. Czerwinka,[1] P. J. King,[1] S. Misat,[1,2] R. P. Campion,[1] C. R. Staddon,[1] and J. C. Villégier[2]
[1]*School of Physics and Astronomy, University of Nottingham, Nottingham NG7 2RD, England*
[2]*Laboratoire de Cryophysique, SPSMS-CEA, 17 rue de Martyrs, 38054, Grenoble, cedex 9, France*
(Received 21 June 2001; revised manuscript received 17 December 2001; published 23 April 2002)

We examine the electrical transport behavior close to vortex ''phase-transition-like'' region in $YBa_2Cu_3O_{7-\delta}$ films that have their *c* axes tilted from the film plane normal by angles of 0°, 5°, 10°, and 15°. The *I-V* isotherms for all films collapse accurately under the vortex-glass scaling algorithm, for magnetic fields of 0.01–1 T applied at angles θ of 0° to 90° with respect to the *c* axis. The critical exponent ν lies in the range 1.3–1.7 for all films, field strengths and field orientations. The critical exponent *z* is magnetic-field strength dependent in all films and for $\mathbf{B}\|\mathbf{c}$ is considerably larger for the group of tilted films than for the 0° film. *z* varies with magnetic-field angle in an opposite sense in the 0° film and in the group of tilted films. The ''transition'' temperatures, $T_t(B,\theta)$, are broadly described by the expression $(T_c-T_t)/T_t \propto (\varepsilon_\theta B)^\beta$, where $\varepsilon_\theta = [\cos^2(\theta)+\varepsilon^2\sin^2(\theta)]^{1/2}$ and $\varepsilon=(m_{ab}/m_c)^{1/2}$. However, $\beta\cong 1/2$, for the 0° film while $\beta\approx 1$ for the group of tilted films. Thus, we find that the tilted films have a number of common behaviors that are quite distinct from those of the 0° film, indicating a dependence of the ''phase-transition-like'' behavior on film structure. The high and variable values of *z* and the lack of ''universality'' between film types does not allow an interpretation of the accurate *I-V* collapses as being evidence for a continuous equilibrium phase transition such as one between a vortex liquid and a vortex glass and we consider models based on flux creep and inhomogenous pinning due to defects.

DOI: 10.1103/PhysRevB.65.184509 PACS number(s): 74.60.Ge, 74.76.Bz, 74.90.+n

I. INTRODUCTION

In the mixed state of the high temperature superconductors (HTS), the combination of high T_c values, small coherence lengths and material anisotropy, gives rise to a rich variety of vortex dynamics and vortex-related phase-transition-like behavior. For HTS materials containing a low density of defects, a first-order transition occurs between the vortex-liquid state and a Bragg-glass state that exhibits algebraic long-range order,[1–3] while at high magnetic fields or for a higher defect density, it is believed a continuous phase transition occurs between the vortex-liquid state and either vortex-glass[4] (VG) or Bose-glass[5] (BG) state depending on the nature of the defect structure.

The supposition of a continuous thermodynamic transition implies associated scaling laws involving ''universal'' critical exponents, under which physical measurements such as *I-V* isotherms may be collapsed onto master curves.[4,5] Over the last decade, many experimental results for $YBa_2Cu_3O_{7-\delta}$ (YBCO) thin films have been presented in the literature in support of a VG transition, this conclusion being based upon the satisfactory collapse of the data under the VG algorithm and the observed ''universality'' for the critical exponent values.[6–10] However, many of these claims for universality are based upon work on *c*-axis normal YBCO films of a similar thickness ($\approx$300 nm). Other work has found that the critical exponents can vary with film thickness[11–13] and track width,[14] while work on 10° tilted *c* axis,[13] *a* axis,[15] and (103) YBCO films[16] has found excellent scaling collapses but very high and variable values of the critical exponent *z*, and even variation of the ''transition temperature'' (T_t) with transport current direction.[15,16] These findings and the ranges of the time and length scales implied by the scaling,[12,13,15,16] have raised doubts concerning the interpretations of scaling collapses as being evidence of ''critical'' behavior and of a continuous thermodynamic liquid-glass phase transition.[17,18] Other authors have considered that the data is evidence for a percolation transition.[19–21] However a true percolative transition constitutes a continuous phase transition with ''universal'' scaling exponents; this interpretation too is subject to the same problems.

A number of authors[17,18,22,23] have considered models for the dissipation based on flux flow[24] and thermally activated flux creep[25,26] but with spatially inhomogeneous distributions of local critical currents. They show that these very simple models predict current-voltage characteristics that appear to collapse under the scaling of the VG algorithm.[17,18,22,23] While VG scaling is a convenient way to characterize the data there is then no real phase transition. The ''transition temperature'' is actually an artifact and the scaling exponents *z* and ν are no longer required to be ''universal'' but become functions of the inhomogeneous defect distribution. Any judgement on whether the vortices are in a liquidlike or solidlike phase is a matter of time scale. However, it is not yet clear whether the quality of scaling collapse offered by these models is comparable to some of the excellent scaling collapses observed experimentally[16] and further work needs to be done on relating the pinning homogeneities to the scaling parameters and thus to experimental data.

The present paper considers the electrical dissipation occurring close to the phase-transition-like region of the high-temperature superconductor YBCO and examines the effects of magnetic field, magnetic-field angle, and tilt of the crys-

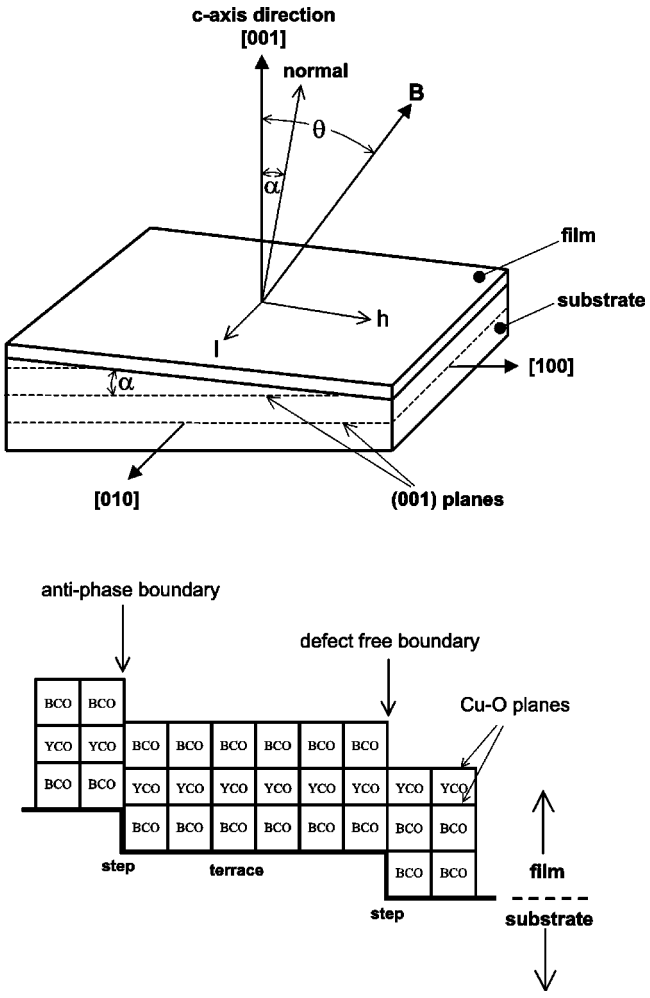

FIG. 1. The upper diagram shows the crystallographic orientations of a vicinal-cut (001) substrate surface and the *c* axis of an YBCO film grown upon it. The transport current directions *l* and *h* are shown. The lower diagram shows the step and terracing at the substrate surface and illustrates antiphase boundaries in the YBCO growth.

tallographic axis of the film. We examine the *I-V* data obtained from four 280-nm-thick YBCO films with different crystallographic orientation. The *c* axis of the films is either normal to the substrate plane (0° film) or tilted away from the substrate normal by 5°, 10°, or 15°. The variation in tilt is achieved by growing the films on vicinally cut $SrTiO_3(001)$ substrates. Figure 1 shows the geometry of these vicinal substrates. The vicinal ''miscut'' orientation is away from the (001) plane and rotated about the [010] direction by angles (α) of 0°, 5°, 10°, and 15°.

The film structure of films grown upon 0° and vicinal substrates are quite different. On 0° substrates, *c*-axis film growth is known to proceed by two-dimensional (2D) or 3D island formation,[27–29]which encourages screw dislocations and spiral growth features.[30,31] However, the ''terrace and step'' surface structure of vicinal substrates encourages step-flow film growth and a suppression of spiral growth,[32–34]with antiphase boundaries and stacking faults forming above the steps to relieve the mismatch between substrate and film. These defects may partially grow out as the film thickens.[32] The growth of YBCO films upon vicinal cut $SrTiO_3(001)$, therefore, enables us to compare the *I-V* behavior of a *c*-axis normal film with films of variable in-plane anisotropy and structure differences.

For each film type $I\text{-}V(B,\theta,T)$ measurements have been taken for orthogonal track directions over a range of temperatures and in applied magnetic fields of 0.01–1 T with $\mathbf{B}\|\mathbf{c}$ and at field angles $0-90°$ (see Fig. 1) with respect to the *c* axis in a field of 1 T. In each case the scaling of the data under the VG scaling algorithm has been used to extract values for the ''transition temperature'' T_t and for the critical exponents ν and *z*.

We find the *I-V* isotherms for the *c*-axis normal and the group of tilted films reveal a number of quite different behaviors when analyzed using the VG scaling algorithm. For all films and magnetic fields we find that the exponent ν is broadly in line with previously published values for *c*-axis normal films with $\mathbf{B}\|\mathbf{c}$. The exponent *z* for our *c*-axis normal (0°) film with $\mathbf{B}\|\mathbf{c}$ is also comparable with other findings, and broadly in line with the predictions of VG theory. However, for the tilted films, the *z* values are considerably higher in magnitude, and the variation of *z* with magnetic-field angle is *fundamentally* different to that of the 0° film. While $T_t(B,\theta)$ for all films is broadly described by the expression $(T_c-T_t)/T_t \propto (\varepsilon_\theta B)^\beta$, we find quite different values for β between the two film types. Thus although the group of tilted films have common behaviors, these are distinct in a number of important ways from those of the 0° film.

II. EXPERIMENT

Four YBCO films were deposited upon vicinal $SrTiO_3(001)$ substrates, miscut at angles 0°, 5°, 10°, and 15° (Fig. 1), using an inverted cylindrical magnetron sputtering technique. Film deposition lasted for 120 min at a substrate temperature of 820 °C in gas pressures of $P_aO_2 = 0.5$ mbars and $P_aAr = 0.3$ mbars. Following deposition the films were annealed at 450 °C in O_2 at a pressure of 850 mbars for 40 min, before cooling to room temperature.

The YBCO orientation and grain alignment of the films were examined from θ-2θ and ω rocking scans obtained using a *Philips PW3710* based diffractometer. The θ-2θ scans for all four samples revealed strong YBCO (00*l*) (*c*-axis orientation) reflections perpendicular to the $SrTiO_3$ (00*l*) planes; the *c* axis, therefore, being tilted away from the substrate normal by the miscut angle. For the 0° film, a small fraction ($\approx 6\%$) of *a*-axis orientation was detected, while for the films grown upon vicinal substrates, only *c*-axis orientation was detected. Full width at half maximum (FWHM) values of the YBCO (005) peaks of 0.10°, 0.28°, 0.30°, and 0.34° for the miscut angles 0°, 5°, 10°, and 15° respectively indicate an increasing strain within the film structure. The FWHM values of the ω scans at the YBCO (005) peak also increase with increasing miscut angle, with values 0.24°, 0.43°, 0.52°, and 0.62° for the 0°, 5°, 10°, and 15° films, respectively, these indicating an increasing misalignment of crystal grain structure.

Silver contact pads were evaporated onto the films before

TABLE I. Normal state properties.

Film	Track	Resistivity $\rho(\mu\Omega\text{cm})$ (100 K)	Anisotropy ρ_h/ρ_l (100 K)	$\rho(T)=A+BT$ A ($\mu\Omega$cm)	B ($\mu\Omega$cm/K)	$T_c(midpoint)$ (K)	ΔT_c (K)
0°	l	128.7	1.0	11.7	1.17	88.40	1.2
	h	128.7		11.7	1.17	88.40	1.2
5°	l	80.6	1.6	−12.4	0.93	90.35	0.65
	h	129.7		6.7	1.23	90.45	0.9
10°	l	80.4	2.9	−14.6	0.95	90.75	0.6
	h	233.6		58.6	1.75	90.90	0.8
15°	l	82.3	4.6	−17.7	1.00	90.26	0.7
	h	377.5		121.5	2.56	90.36	0.9

two perpendicular measurement tracks were formed using conventional UV lithography and wet etching using 0.8% concentration orthophosphoric acid. The track geometry was of the usual four-point-type, with a track width of 50 μm and track length of 5000 μm between voltage points. The orientation of the tracks with respect to the film plane and the substrate crystallographic axes are shown in Fig. 1. One track, which we will refer to as "*l*," lies parallel to the substrate [010] direction and at right angles to the track that we will refer to as "*h*."

Cryogenic dc electrical measurements were made using an *Oxford CF200* cryostat. A *Keithley 220* current source enabled transport currents in the range 1 nA–100 mA to be passed through either of the tracks. The voltage terminals of the tracks were connected directly to a low noise battery operated *EM Electronics A10* nanovoltage amplifier (gain 3880) and the output measured using a *Keithley 195* voltmeter. A magnetic field of up to 1 T could be applied to the sample at orientations 0–360° with respect to the sample normal [see Fig. 1].

Families of *I-V* isotherms were obtained for each sample in fields ranging from 0.01–1 T ($\mathbf{B}\|\mathbf{c}$) and at field angles 0–90° with respect to the *c* axis in a 1 T magnetic field. Each *I-V* family contained typically ≈60 isotherms encompassing a range of temperatures from T_c to well below the "transition temperature" T_t, the temperature at which the curvature passes from from positive to negative. We used a temperature drift criterion of ± 0.5 mK between consecutive data points of each *I-V* curve that gave a maximum temperature drift of typically 10 mK between all data points of a single curve. The noise level of our system was sufficiently low to allow voltage measurements down to 1 nV.

III. RESULTS

A. Normal-state properties

Numerical data for the normal-state properties of the four films are shown in Table I. It may be seen that the midpoint transition temperature T_c of the 0° film is a little lower than those of the tilted axis films and the transition width ΔT_c is somewhat greater, probably due to a greater defect density. However T_c and ΔT_c for the vicinal films are close to the optimal values observed for YBCO films.

The resistivities of all the films are metallic when measured along the *l* direction; the data can be fitted to the expression $\rho(T)=A+BT$, and the low values of A show that $\rho(T)$ extrapolates close to the origin. This direction corresponds to transport along the *ab* planes, and the lower ρ_l magnitudes observed for the tilted films indicate a lesser disruption of the *ab* structure than for the 0° film. For high quality YBCO untwinned single crystals, values of $\rho_a \approx 45$ $\mu\Omega$cm, $\rho_b \approx 25$ $\mu\Omega$cm ($T=100$ K) have been reported,[35] these being significantly lower than the values typically observed for YBCO film systems. Lemberger[36] reports $\rho_{ab}=70$–120 $\mu\Omega$cm for films grown on $SrTiO_3(001)$ 0° substrates, Haage *et al.*[32] report $\rho_{ab}=57$ $\mu\Omega$cm for a 320-nm-thick film grown on 10° vicinal $SrTiO_3(001)$, and Campion *et al.*[16] report $\rho_{ab}=40-48$ $\mu\Omega$cm for (103) films grown on vicinal $SrTiO_3(011)$ substrates.

Our figures for the *l* tracks of the tilted films are higher than those of Haage *et al.* and Campion *et al.*, but close to the lower limit of Lemberger's range. The figure for the 0° film is at the upper limit of Lemerberger's range, influenced by the *a*-axis inclusions. The data for the *h* tracks shown in Table I reveals the increasing influence of the higher resistance *c*-axis direction for increasing film tilt. The anisotropies shown in Table I may be compared with the figures of 1, 1.6, 3.5, and 5.7 for the 0, 5, 10, 15° films, respectively, which may be derived for a tilted single crystal with a c/ab anisotropy of 85.[32] It may be seen that, as the tilt increases, the observed anisotropy falls below the ideal value, indicating an increased degree of crystalline disorder with increased tilt.

B. *I-V* scaling under the *VG* algorithm

The families of *I-V* isotherms from the superconducting region of all four samples were analyzed using the VG scaling algorithm.[4] At temperatures in the vicinity of the vortex-glass transition it is proposed that the behavior of the system can be described by a diverging length scale and a diverging time scale, varying as $|T-T_{VG}|^{-\nu}$ and $|T-T_{VG}|^{-z\nu}$, respectively, where T_{VG} is the vortex-glass transition temperature and ν and z are defining critical exponents. Dimensional considerations then allows *I-V* data to be related to the parameters T, T_{VG}, ν, and z by the VG scaling algorithm,

$$(V/I)|T-T_{VG}|^{-\nu(z-d+2)}=F_{\pm}I|T-T_{VG}|^{-\nu(d-1)}. \quad (1)$$

Here $d(>2)$ is the dimensionality of the system and $F_{\pm}$ are universal functions for temperatures above $(+)$ and below $(-)$ T_{VG}. A family of I-V isotherms plotted as V/I vs I with the axis scaled by $|T-T_{VG}|^{-\nu(z-d+2)}$ and $|T-T_{VG}|^{-\nu(d-1)}$, respectively, should then overlay to map out the functions $F_{\pm}$ for temperatures above and below T_{VG}, respectively.

Custom written computer software was used to plot the scaled data in $\log_{10}(V/I)$ vs $\log_{10}(I)$ form in order to obtain values for the transition temperature T_t and the critical exponents ν and z on the supposition that $d=3$. The following procedure was adopted: First, approximate values for T_t and z were found by noting the temperature and the gradient of the isotherm that most accurately displayed power-law behavior. At the transition temperature the gradient is given by $(z+1)/(d-1)$ that enables a value for z to be deduced. These initial values, together with a trial value for ν were used to scale all isotherms of the data set, with subsequent iterative rescaling making small adjustments to ν, z, and T_t, until we obtained a ''best-fit'' collapse of the data onto two master curves.

Figure 2 shows a typical family of I-V isotherms before and after the scaling procedure. It may be seen that the data from a region of temperature extending both above and below the transition temperature T_t collapses extremely well onto the two master curves F_+ and F_-. Above an upper temperature T_U the collapse fails abruptly. At T_U the resistivity is typically 1% of the value at T_c (midpoint). Below a lower temperature T_L the collapse gradually worsens. It is possible to collapse the data for all films, magnetic fields, and field angles in this way, to obtain a typical precision of ± 0.2 K in T_t, $\pm 8\%$ in the exponent z and $\pm 10\%$ in the exponent ν.

C. Variation of the scaling exponents with magnetic field

We find that the critical scaling exponent ν exhibits no strong variation with film type or with magnetic-field angle and shows no significant differences between the two tracks that lie outside the experimental error. In all cases, ν values lie within the theoretical predicted range of 1–2.[4,6] ν typically increases by about 0.2 between very low fields and 0.03 T while at higher fields it remains relatively constant within the range 1.5 ± 0.2 for all films.

The exponent z also shows no significant variations between measurement tracks except for the 10° and 15° films where there are differences at levels of 2–3 standard deviations. z, however, exhibits strong variations as a function of both magnetic-field strength and field orientation. As a function of magnetic-field strength and for $\mathbf{B}\|\mathbf{c}$, $z(B)$ for the 0° film falls from 9.5→6.5 as the field is increased from 0.01 →1 T. For the 5°, 10° and 15° tilted films, the corresponding $z(B)$ variations across fields of 0.01→1 T, are approximately 17→12, 17→12, and 16→15, respectively. The only agreement with the VG prediction of $z\approx 4-7$ (Refs. 4 and 6) is for the 0° film in fields above 0.6 T. Despite these magnitude differences of $z(B)$ for the film types, in all films $z(B)$ decreases with increasing field strength. However, we

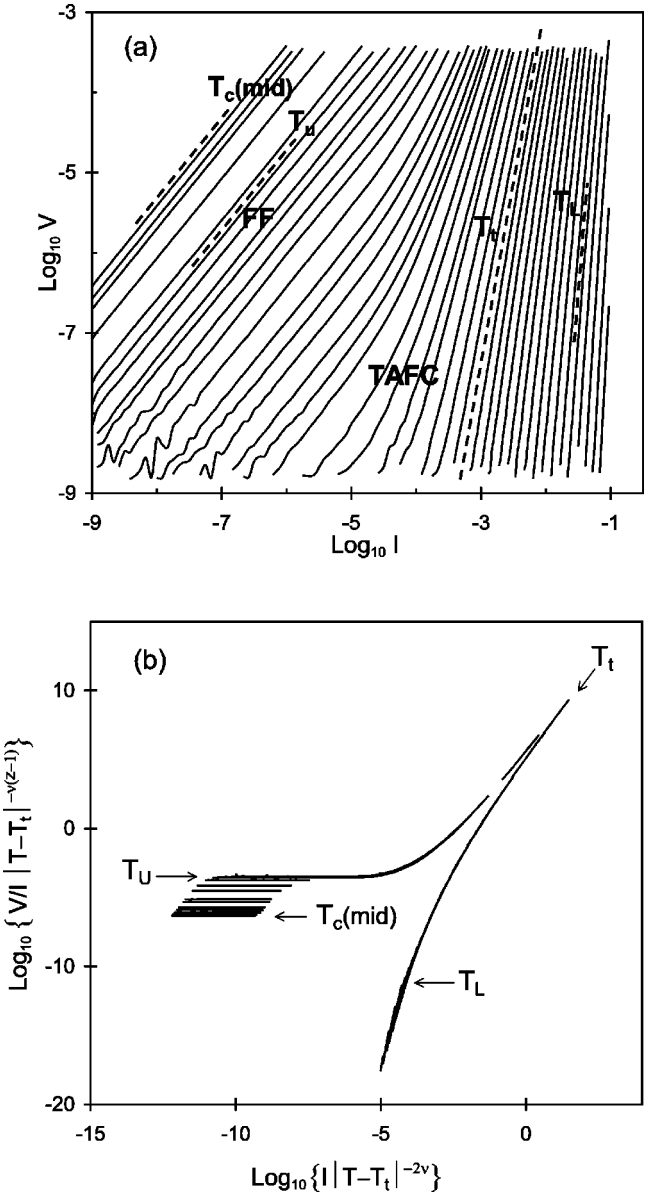

FIG. 2. (a) Typical family of $\log_{10}(V)$ vs $\log_{10}(I)$ isotherms showing the flux–flow (FF) and thermally activated flux creep regimes (TAFC), the midpoint of the normal-superconducting transition T_c(mid), the ''critical'' isotherm displaying linear behavior T_t, and typical upper (T_U) and lower (T_L) temperature of the isotherms for which good scaling collapse is observed. (b) The data of (a) in the form $\log_{10}(V/I)$ vs $\log_{10}(I)$ collapsed under the VG scaling algorithm.

find fundamental differences between the 0° film and the group of tilted films for the dependence of $z(\theta)$ upon magnetic-field orientation. Figure 3(a) shows, for the 0° film, the variation of z with field angle for a magnetic field of 1 T. z increases smoothly from values of 6.5 ± 0.3 for $\mathbf{B}\|\mathbf{c}$ to 7.8 ± 0.6 for $\mathbf{B}\|(\mathbf{a,b})$. Figure 3(b) shows the corresponding data for the 5° film. Here z *falls* with increasing angle from values of around $z=12$ at $\mathbf{B}\|\mathbf{c}$ to around $z=8$ for $\mathbf{B}\|(\mathbf{a,b})$. The results for the 10° and 15° films are of a similar form. For the 10° film z falls from around $z=12$ at $\mathbf{B}\|\mathbf{c}$ to around $z=9$ at $\mathbf{B}\|(\mathbf{a,b})$. For the 15° film z falls from around z

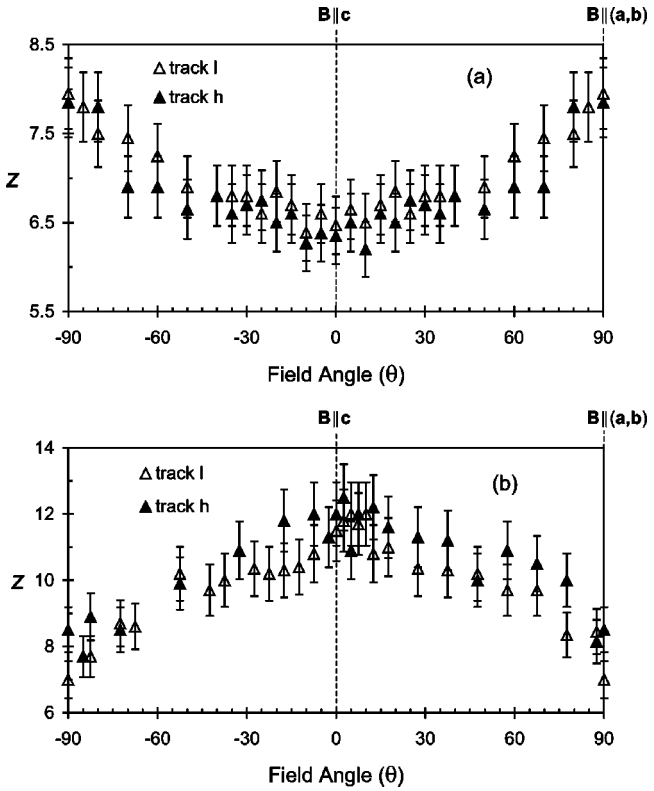

FIG. 3. Variation of the scaling exponent z with magnetic-field angle for (a) the 0° film and (b) the 5° film. A magnetic field of 1 T was used in each case.

$=15$ at $\mathbf{B}\|\mathbf{c}$ to around $z=11$ at $\mathbf{B}\|(\mathbf{a,b})$. Thus the trends of z with changing magnetic-field angle in the 5°, 10°, and 15° films are *fundamentally* different from that of the 0° film.

D. Variation of T_t with magnetic field

Using the scaling procedure described earlier, we have obtained values for $T_t(B,\theta=0)$, as a function of field strength (at 0.01, 0.03, 0.1, 0.3, 0.6, and 1 T) at the field orientation $\mathbf{B}\|\mathbf{c}$ for each tilt of film. We have also obtained values for T_t as a function of the magnetic-field angle θ with respect to the c axis, using a fixed magnetic-field strength of 1 T. In analyzing this data we compare our results with the prediction for the melting temperature (T_m) of a vortex lattice based on the Lindemann melting criterion,[37] which for an anisotropic material is given by[38]

$$T_m(B,\theta)\cong\frac{\varepsilon c_L^2\phi_0^{5/2}}{\mu_0\pi k_B\lambda^2(T)(\varepsilon_\theta B)^{1/2}}. \tag{2}$$

Here $\varepsilon=(m_{ab}/m_c)^{1/2}$ is the effective-mass anisotropy with $\frac{1}{7}<\varepsilon<\frac{1}{5}$,[38] and $\varepsilon_\theta=[\cos^2(\theta)+\varepsilon^2\sin^2(\theta)]^{1/2}$ is the angular dependent anisotropy parameter, where θ is the field angle with respect to the c axis. The Lindemann parameter c_L is the fraction of the lattice parameter (a_o) that a vortex line is considered to deviate from equilibrium to define a vortex lattice ''melting'' and is expected to lie in the range 0.1–0.2.[38] If the temperature dependence of the magnetic penetration depth takes the form $\lambda_{ab}^2(T)=\lambda_{ab}^2(0)T_c/(T_c-T)$, then Eq. (2) may be written as

$$\frac{T_m(B,\theta)}{T_c-T_m(B,\theta)}=\frac{\varepsilon c_L^2\phi_0^{5/2}}{\mu_0\pi k_B\lambda_{ab}^2(0)T_c(\varepsilon_\theta B)^\beta}, \tag{3}$$

where $\beta=1/2$.

$T_m(B,\theta)$ then takes the form

$$T_m(B,\theta)=\frac{T_c}{1+\alpha(\varepsilon_\theta B)^\beta} \tag{4}$$

with $\alpha=\mu_0\pi k_B\lambda_{ab}^2(0)T_c/\varepsilon c_L^2\phi_0^{5/2}$.

We have fitted our experimental $T_t(B=1\ \mathrm{T},\theta=0)$ data to Eq. (4). The resulting values of α, β, and T_c for the four films are given in Table II. In all cases the fitting quality is satisfactory allowing for the errors of ±0.2 K in our values of T_t. The values of T_c lie in each case at about 0.9 K lower than the midpoint values given in Table I. For the 0° film the value of β is very close indeed to the value of 0.5 of the Lindemann vortex-lattice melting model, corresponding to a $(T_c-T_t)/T_t\propto B^{0.49}$ dependence [Eq. (3)]. A similar dependence to this has been observed for the vortex-lattice melting in ''clean'' YBCO crystals.[39,40] Other workers[41,42] report values of β close to 0.7 for similar crystal samples, while for c-axis films, β in the range 0.66–0.75 has been observed,[6,43]often for much larger magnetic-field strengths than our own. For the tilted films we find a quite different dependence to that of the 0° film. The tilted films have a common behavior, the β values all lying within the range $\approx1.0\pm0.1$, giving $(T_c-T_t)/T_t\propto B$.

Figure 4(a) shows $T_t/(T_c-T_t)$, plotted as a function of θ, for the 0° film. Our experimental $T_t(\theta)$ values for this film were obtained for field angles in the range $-10°$–95°, but the geometrical symmetry for this film allows us to use these values to form the $-120°$–$+120°$ angular plot shown. The data is compared with the angular predictions of Eq. (3), using $\lambda_{ab}(0)=1400$ Å, and $T_c=87.17$ (Table II). We find that $\varepsilon=0.20$, and $c_L\cong0.20$ provide the best overall fit to the data. This value for the Lindemann parameter is physically reasonable and compares favorably with the range of values expected for vortex-lattice melting of $c_L=0.1-0.2$.[38] It may be seen that the experimental data is in broad agreement with the prediction of Eq. (3) with an accurate agreement for angles $\theta\gtrsim40°$ but with some discrepancy for $\theta\lesssim40°$. We

TABLE II. Parameters obtained by fitting the $T_t(B)$ ($\mathbf{B}\|\mathbf{c}$) data to Eq. (4).

Film	Track	α	β	T_c
0°	l	0.052	0.49	87.17
5°	l	0.057	0.87	89.46
	h	0.056	0.94	89.33
10°	l	0.053	1.10	89.74
	h	0.064	0.90	89.93
15°	l	0.078	1.06	89.35
	h	0.077	1.04	89.49

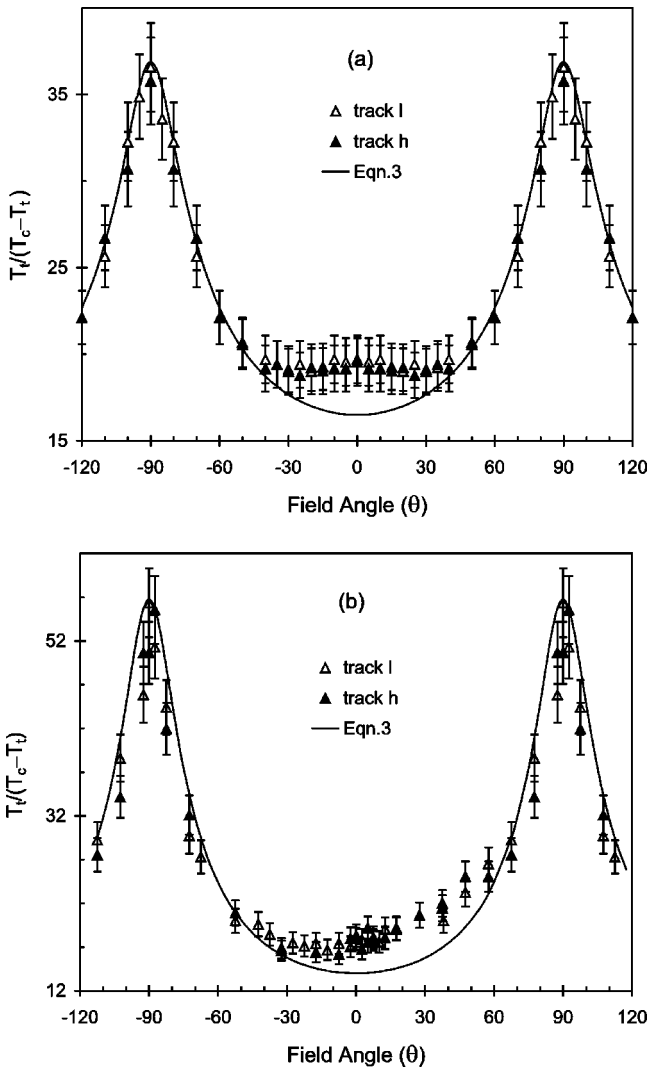

FIG. 4. Experimental T_t data plotted as $T_t/(T_c-T_t)$ vs magnetic-field angle (θ) for, (a) the 0° film and (b) the 5° film, measured in a field of 1 T. The continuous lines are the predictions of Eq. (3) using the parameters described in the text.

should consider whether this behavior, where T_t remains relatively constant or possibly reduces slightly as the field is tilted away from the *c* axis before rising for angles $\theta \gtrsim 40°$, is indicative of Bose-glass behavior. The Bose-glass model considers linelike or planar pinning effects upon the vortex system and predicts a lowering of the BG transition temperature T_{BG} when the applied field is tilted away from such defects. This might arise from strong vortex pinning at *a-b* twin boundaries aligned parallel to the *c* axis. BG like behavior in a thick (1000 nm) YBCO *c*-axis film has been reported by Safar *et al.*[44] who observed a distinct reduction of T_t with field tilt (0°–30°) away from the *c* axis. They quote exponent values of $\nu' = 1.3 \pm 0.1$ and $z' = 6.3 \pm 0.3$, these comparing favorably with $\nu' = 1 \pm 0.1$ and $z' = 6 \pm 0.5$ expected from Bose-glass theory.[5](Note: BG and VG exponents are related by $\nu' = 2/3\nu$ and $z' = 1/2(3z+1)$). If we interpret our data using BG and VG scaling we obtain exponents values (at $\mathbf{B} \| \mathbf{c}$) of $\nu' = 1.2 \pm 0.1$, $z' = 10.3 \pm 1.0$ and $\nu = 1.8 \pm 0.1$, $z = 6.5 \pm 0.5$ respectively. Thus our "*z*" values are far higher than those of Safar *et al.* and are in closer agreement with those expected of VG predictions; we have no unambiguous evidence for the existence of a Bose-glass transition in our film.

Figure 4(b) shows a similar comparison between the data for the 5° film and the angular prediction of Eq. (3). However, we note from Table II that the magnetic-field dependence of $T_t(B, \theta = 0)$ for this film does not follow the expectation of the model. Therefore to extract a value for the Lindemann parameter by fitting Eq. (3) to this data would be unsound. Rather we have presented the angular dependence in Fig. 4(b) by using the angular dependence of Eq. (3), together with the appropriate values of β, scaling the magnitude of the prediction to give the best overlay. The overall agreement using, $\varepsilon = 0.2$ and T_c values from Table II [for the $T_t/(T_c - T_t)$ term], is seen to be good, although it is evident there is slight asymmetrical angular dependence of the $T_t(\theta)$ data. There is no evidence of BG behavior in this film, the general trend being a smoothly varying $T_t(\theta)$ as a function of field angle. Similar asymmetrical behaviors and field angle dependencies are found for the 10° and 15° films.

In summary we observe that the angular dependence of T_t for all films may be generally described by the expression $(T_c - T_t)/T_t \propto (\varepsilon_\theta B)^\beta$. However, only the 0° film, with $\beta \cong 1/2$, shows the dependence upon magnetic-field magnitude in accordance to the Lindemann critereon; the group of tilted films having quite different dependences with $\beta \approx 1$.

IV. DISCUSSION

The vortex melting transition has a dramatic influence on the electrical behavior of HTS thin films, producing what appears to be the signature of a higher-order phase transition, with a magnetic-field-dependent transition temperature T_t separating ohmic small-current behavior at $T > T_t$ from nondissipative small-current behavior at $T < T_t$. This transition is closely related to the "irreversibility" line of magnetic studies, which also indicates a transition from an essentially mobile state, to a state in which the vortices are far less mobile.

The "transition" observed in thin-film systems certainly show none of the characteristic features of first-order behavior. An interpretation of the phenomenon as a continuous equilibrium phase transition, such as one between a vortex-liquid and a vortex-glass phase, leads to the scaling algorithm, which we and others have described. Within the limitations of the assumptions being made, which include aspects of the defect topology, there is also an expectation that the same scaling exponents will be found for different specific superconductors, for different geometries, for different defect structures and for different magnetic fields. This is the expectation for a "universal" phase transition. Scaling collapses under this algorithm have been widely observed both for HTS single crystals and for a range of HTS thin-film systems, and these observations have been used to justify the assumption of a continuous thermodynamic phase transition based on the "melting" of a vortex glass. Scaling collapses under the VG algorithm are common; in some cases they are

spectacularly good,[16] collapsing data taken over very wide ranges of temperature.

However, many aspects of this interpretation cause a number of concerns. These concerns include the lack of universality of the scaling exponents, the very high values of the exponent z found in film systems other than c-axis normal[13,15,16] and the variation of T_t with transport current direction found in at least two systems.[15,16] The inability, at least in electrical transport measurements, for the collapse to fail as T_t is approached, leads to absurdly large ranges of the length and time scales of the problem on this interpretation. At the same time, experimental evidence for critical slowing is sparse, and some argue, that vortex-glass transitions should not exist even in three dimensions once screening has been correctly treated.[45]

In the present paper we have examined the ''transition'' behavior in YBCO thin films of the same thickness, and track geometry, but with two quite distinctive structures. c-axis normal films exhibit a defect structure with stress relief via twinning and spiral growth while the films grown on vicinal substrates exhibit a different defect structure, the stress relief occurring via the formation of stacking faults and the antiphase boundaries that originate from the substrate terrace-step structure.

We observe good scaling collapses in all of our films over the magnetic-field range 0.01–1 T, and from these collapses obtained sets of values of ν, z, and T_t. It is clear that the films grown upon tilted substrates share a number of common properties, which differ from those of the c-axis normal film. While the values for the exponent ν show some ''universal'' behavior for all films, the magnitude of exponent z is markedly different between the 0° film and tilted films while the $z(\theta)$ dependence on field angle is *fundamentally* different between the two film types. Further differences between the film types are found in both the field angle and field strength dependence of the transition temperature T_t.

These findings are not compatible with the idea of a ''universal'' continuous equilibrium transition between a vortex-liquid and a vortex-glass for both film systems. It is clear that an alternative model is required, one which offers the scaling of the data onto two branches as in continuous equilibrium phase-transition models, but one that is not dependent upon the same assumptions concerning length and time scales and also one which does not require the assumption of universal behavior.

One early theory of the transition in the electrical transport behavior was the ''parallel resistor'' model of Greissen,[22] who combined the flux-flow model of Bardeen and Stephen[24] with the thermally activated flux creep model of Anderson and Kim,[25,26] extending the latter to include a distribution of activation energies. He found a kink in the temperature dependence of the power-law exponent $\alpha(T)$ occurring in the power law expression $V \propto I^{\alpha}$, without this being any way an indication of phase-transition behavior. Later authors have examined the current-voltage characteristics predicted by models that include flux flow, thermally activated flux creep, and spatially inhomogeneous distributions of pinning barriers or the equivalent in the form of local critical currents. The predictions have then been subjected to scaling under the VG algorithm.[17,18,23,46] It is found that the data scales under this algorithm to some degree without in any way implying a true phase transition. The appearance of a transition is an artifact and z and ν are not universal scaling exponents. Rather T_t, z, and ν are parameters of the particular model, each dependent upon details of the inhomogeneous distributions of pinning strengths and other factors.

Such models overcome the problems associated with the observed sample and magnetic-field-dependent values of z, and with considerations of length and time scales. It is easy to modify such models to include anisotropic pinning, in which case there are circumstances in which the ''transition temperature'' would vary with the angle of the applied transport current. The Bose-glass situation could be dealt with in analogous way by incorporating barriers dependent on the magnetic-field lines and the local low-dimensional defect structure. At present these models are not yet fully developed. The way in which they include the material properties is simplistic. It is not clear that all treatments of the inhomogeneities are consistent with the topological constrains imposed by the vortex movement across the sample that leads to the dissipation. Nor have investigations been fully extended to identify those distributions of inhomogeneties that would lead to acceptable qualities of scaling collapse, and to consider whether such models can indeed lead to the excellent scaling observed in some thin-film systems, and whether these distributions correspond to those deduced from experimental investigations such as magnetic measurements. However, such models lead directly to relationships between the parameters such as z and details of the pinning distributions. Matsushita *et al.*[17] report that, in their model, z decreases as the inhomogeneity of flux-pinning strength is increased.

It is important to note that it is the inhomogeneity of the flux pinning on the spatial scale of a flux bundle that determines z in these models rather than the strength of the pinning itself. Unfortunately very little is known about the degree of inhomogeneity in most HTS systems. However there is some evidence to support Matsushita *et al.*'s relationship between inhomogeneity and z. The dramatic lowering of z when a 10° YBCO thin film was subject to chemical etching[13] is certainly consistent with this prediction. It is plausible to suppose that the inhomogeneity in the pinning is greater for films with certain classes of defect, including c-axis normal films with their extended twin boundaries and screw dislocations, rather than for films on vicinal substrates where the twinning may be suppressed[47] and screw dislocations absent. It is also plausible to suppose that inhomogeneity is greater for the higher defect densities found in thicker films. These suppositions would then provide an explanation for the findings of Sawa *et al.*[11] who report that z is lower in c-axis normal films of greater thickness and for a number of features found in our own experiments. It is most revealing that while there is a large discrepancy in z values ($\approx 6.5 - 15$) for $\mathbf{B} \| \mathbf{c}$ between our c-axis normal and tilted films, for $\mathbf{B} \| (\mathbf{a},\mathbf{b})$ z values lie in a far narrower range ($\approx 8 - 11$). For this field orientation there is strong intrinsic pinning of vortices lying between the ab planes, therefore, the pinning in-

homogeneity will be similar between the film types hence the observed narrow range of z values. However the models that relate z with pinning inhomogeneity are not at present based on firm foundations due to a lack of knowledge of pinning strength inhomogeneity in HTS.

Although we do not rule out the possibility of a vortex liquid-to-glass phase transition for specific classes and systems of HTS materials, our experimental findings in this present work do not provide firm evidence for this phase transition.

ACKNOWLEDGMENTS

We are grateful to the Engineering and Physical Sciences Research Council (EPSRC) for a maintenance grant (PSC), and to K.A. Benedict, R.M. Bowley, and M.R. Swift for helpful discussions.

[1] T. Giamarchi and P. L. Doussal, Phys. Rev. B **52**, 1242 (1995).
[2] T. Giamarchi and P. L. Doussal, Phys. Rev. B **55**, 6577 (1997).
[3] T. Nishizaki and N. Kobayashi, Supercond. Sci. Technol. **13**, 1 (2000).
[4] D. S. Fisher, M. P. A. Fisher, and D. A. Huse, Phys. Rev. B **43**, 130 (1991).
[5] D. R. Nelson and V. M. Vinkour, Phys. Rev. B **48**, 13 060 (1993).
[6] R. H. Koch, V. Foglietti, W. J. Gallagher, G. Koren, A. Gupta, and M. P. A. Fisher, Phys. Rev. Lett. **63**, 1511 (1989).
[7] J. Kötzler, G. Nakielski, M. Baumann, R. Behr, F. Georke, and E. H. Brandt, Phys. Rev. B **50**, 3384 (1994).
[8] P. J. M. Wöltgens, C. Dekker, J. Swüste, and H. W. d. Wijn, Phys. Rev. B **48**, 16 826 (1993).
[9] J. Deak, M. McElfresh, R. Muenchausen, S. Foltyn, and R. Dye, Phys. Rev. B **48**, 1337 (1993).
[10] P. J. M. Wöltgens, C. Dekker, S. W. A. Gielkens, and H. W. d. Wijn, Physica C **247**, 67 (1995).
[11] A. Sawa, H. Yamasaki, Y. Mawatari, H. Obara, M. Umeda, and S. Kosaka, Phys. Rev. B **58**, 2868 (1998).
[12] S. Misat, P. J. King, D. Fuchs, J. C. Villégier, P. S. Czerwinka, and R. P. Campion, Physica C **330**, 72 (2000).
[13] P. S. Czerwinka, R. P. Campion, K. F. Horbelt, P. J. King, S. Misat, S. M. Morley, H.-U. Habermeier, and B. Leibold, Physica C **324**, 96 (1999).
[14] Y. Ando, H. Kubota, and S. Tanaka, Phys. Rev. Lett. **69**, 2851 (1992).
[15] S. Misat, P. J. King, D. Fuchs, J. C. Villégier, R. P. Campion, and P. S. Czerwinka, Physica C **331**, 241 (2000).
[16] R. P. Campion, P. J. King, K. A. Benedict, R. M. Bowley, P. S. Czerwinka, S. Misat, and S. M. Morley, Phys. Rev. B **61**, 6387 (2000).
[17] T. Matsushita, T. Tohdo, and N. Ihara, Physica C **259**, 321 (1996).
[18] B. Brown, Phys. Rev. B **61**, 3267 (2000).
[19] K. Yamafuji and T. Kiss, Physica C **258**, 212 (1996).
[20] M. Ziese, Phys. Rev. B **53**, 12 422 (1996).
[21] M. Ziese, Physica C **269**, 35 (1996).
[22] R. Griessen, Physica C **175**, 315 (1991).
[23] T. Sueyoshi, N. Ishikawa, A. Iwase, Y. Chimi, T. Kiss, T. Fujiyoshi, and K. Miyahara, Physica C **309**, 79 (1998).
[24] J. Bardeen and M. J. Stephen, Phys. Rev. **140**, 1197 (1965).
[25] P. W. Anderson, Phys. Rev. Lett. **9**, 309 (1962).
[26] P. W. Anderson and Y. B. Kim, Rev. Mod. Phys. **36**, 39 (1964).
[27] X.Y. Zheng, D. H. Lowndes, S. Zhu, J. D. Budau, and R. J. Warmack, Phys. Rev. B **45**, 7584 (1992).
[28] S. J. Pennycook, M. F. Chisolm, D. E. Jesson, D. P. Norton, D. H. Lowndes, R. Feenstra, H. R. Kerchner, and J. O. Thompson, Phys. Rev. Lett. **67**, 765 (1991).
[29] S. Zhu, D. H. Lowdnes, X. Y. Zheng, D. P. Norton, and R. J. Warmack, Mater. Res. Soc. Symp. Proc. **237**, 541 (1992).
[30] C. Gerber, D. Anselmetti, J. G. Bednorz, J. Mannhart, and D. G. Schlom, Nature (London) **350**, 279 (1992).
[31] M. Hawley, I. D. Raistrick, J. G. Berry, and R. J. Houghton, Science **251**, 1587 (1991).
[32] T. Haage, J. Zegenhagen, J. Q. Li, H.-U. Habermeier, M. Cardona, C. Jooss, R. Warthmann, A. Forkl, and H. Kronmüller, Phys. Rev. B **56**, 8404 (1997).
[33] R. R. Biggers, M. G. Norton, I. Maartense, T. L. Peterson, E. K. Moser, D. Dempsey, M. A. Capano, J. Talvacchio, J. L. Brown, and J. D. Wolf, IEEE Trans. Appl. Supercond. **5**, 1241 (1995).
[34] L. Méchin, P. Berghuis, and J. E. Evetts, Physica C **302**, 102 (1998).
[35] T. A. Friedmann, M. W. Rabin, J. Giapintzakis, J. P. Rice, and M. Ginsberg, Phys. Rev. B **42**, 6217 (1990).
[36] T. R. Lemberger, *Physical Properties of High Temperature Superconductors III* (World Scientific, Singapore, 1992).
[37] F. Lindemann, Phys. Z. **11**, 69 (1910).
[38] G. Blatter, M. V. Feigel'man, V. B. Geshkenbein, A. I. Larkin, and V. M. Vinkour, Rev. Mod. Phys. **66**, 1125 (1994).
[39] R. G. Beck, D. E. Farrell, J. P. Rice, D. M. Ginsburg, and V. G. Kogan, Phys. Rev. Lett. **68**, 1594 (1992).
[40] D. E. Farrell, J. P. Price, and D. M. Ginsburg, Phys. Rev. Lett. **67**, 1165 (1991).
[41] W. K. Kwok, S. Flesher, U. Welp, V. M. Vinkour, J. Downey, G. W. Crabtree, and M. M. Miller, Phys. Rev. Lett. **69**, 3370 (1992).
[42] D. López, L. Krusin-Elbaum, H. Safar, E. Righi, F. d. l. Cruz, S. Grigera, C. Feild, W. K. Kwok, L. Paulius, and G. W. Crabtree, Phys. Rev. Lett. **80**, 1070 (1998).
[43] L. Hou, J. Deak, P. Metcalf, M. McElfresh, and G. Preosti, Phys. Rev. B **55**, 11 806 (1996).
[44] H. Safar, S. R. Foltyn, Q. A. Jia, and M. P. Maley, Philos. Mag. B **74**, 647 (1996).
[45] C. Wengel and A. P. Young, Phys. Rev. B **54**, 6869 (1996).
[46] K. Yamafuji and T. Kiss, Physica C **290**, 9 (1997).
[47] J. Brötz, H. Fuess, T. Haage, and J. Zegenhagen, Phys. Rev. B **57**, 3679 (1998).